Article

Simulated and Experimental Dispersed-Phase Breakage and Coalescence Behavior in a Kühni Liquid–Liquid Extraction ColumnSteady State

Lusa N. Gomes, Margarida L. Guimares, Pedro F. R. Regueiras, Johann Stichlmair, and Jos J. Cruz Pinto

Ind. Eng. Chem. Res., **2006**, 45 (11), 3955-3968 • DOI: 10.1021/ie051453l

Simulated and Experimental Dispersed-Phase Breakage and Coalescence Behavior in a Kühni Liquid−Liquid Extraction Column−Steady State

Luísa N. Gomes,[†] Margarida L. Guimarães,[†] Pedro F. R. Regueiras,[‡] Johann Stichlmair,[§] and José J. Cruz Pinto*,[||]

Instituto Superior de Engenharia do Porto, Dep. Engenharia Química, Rua Dr. António Bernardino de Almeida 431, 4200-072 Porto, Portugal; Faculdade de Engenharia da Universidade do Porto, Rua Dr. Roberto Frias, s/n 4200-465 Porto, Portugal; Lehrstuhl für Fluidverfahrenstechnik, Technische Universität München, Boltzmannstr. 15, D-85747 Garching bei Munchen, Germany; and CICECO/Dep. Química, Universidade de Aveiro, Campus de Santiago, 3810-193 Aveiro, Portugal

Given the difficulties normally associated with direct experimentation in liquid−liquid extraction processes, their direct computer simulation has acquired increased relevance and utility, especially when dealing with some of the details of the dispersed-phase hydrodynamics. The possibility of testing very complex theoretical models of such behavior is increasingly attractive to the researcher, as a result of both the power and the availability of personal computing resources. Experimental data obtained in a pilot-scale Kühni liquid−liquid extraction column and simulated data generated by means of a drop population-balance model and algorithm were used to describe and compute the local drop-size distributions and dispersed-phase holdup profiles. In this work, the applicability of this algorithm to describe the steady-state behavior of a Kühni liquid−liquid extraction column is illustrated. Data generated using this algorithm exhibit reasonable agreement with experimental data, with physically meaningful model parameter values.

Introduction

It is well-known that solute transfer between two liquid phases, one dispersed and another continuous, is highly dependent on the dispersed-phase hydrodynamics, namely, on the breakage and (interdrop) coalescence processes. We must be able to describe mathematically both the dynamics of the fluid (including the hydrodynamic effects of drop coalescence and breakup) and the mass-transfer mechanisms (which, in turn, depend on the movement of the fluid inside and outside the drops themselves), to simulate the behavior of the system and predict the influence of different operating variables on the extraction efficiency.

Early computer simulations of agitated liquid−liquid systems were based on ad hoc heuristics to describe peculiarly idealized interactions within the dispersed phase. Most of the present approaches, however, employ highly sophisticated models. Among such models, Coulaloglou and Tavlarides' model[1] for the locally isotropic regime enjoys well-deserved prominence; this model, though after some adjustments, has been widely accepted as adequately accurate, when mass transfer is both present and absent, and has been extensively put to use for both stirred vessels and extraction columns.

In recent years, many authors have spent considerable efforts in modeling mechanically agitated devices for liquid−liquid contact and in attempting the experimental validation of their models. Models such as those of Cruz-Pinto,[2] Tsouris et al.,[3] and Gerstlauer et al.[4] have been declared able to describe with reasonable accuracy the results of their authors' experiments, even if many of them adopted significant simplifications—such as ignoring coalescence and/or contemplating the steady state alone—in order to make calculations feasible in reasonable time.

The experimental evidence presented and discussed in earlier works[2,5,6] by this team suggests that, even in agitated liquid−liquid extraction columns, like Kühni columns, interdrop coalescence cannot be neglected. The same applies to simple mixers.[7]

The algorithms for the solution of the population-balance equation (PBE) in dynamic conditions, designed to obtain the drop-size distribution, solute concentrations, and local dispersed-phase holdup profiles along the column height, accounting for drop breakage and coalescence, are very complex and computationally heavy, given the multiple mixing stages of the column (each approximately describable by an ideally agitated vessel) and the intervening interstage flows. Ribeiro et al.[8,9] published innovative stirred-vessel algorithms for directly (numerically) solving the PBE in three-dimensional phase space (drop volume, age, and solute concentration), allowing for both drop breakage and interdrop coalescence processes.

To describe solute mass transfer, these workers adopted either a rigid or an oscillating drop model, as referred to or developed by Cruz-Pinto[2] and Cruz-Pinto et al.,[10] and used Coulaloglou and Tavlarides's[1] drop interaction model (despite two formal errors, identified and commented on further below) to quantify their breakage and coalescence frequencies. This algorithm, as developed for an ideally agitated vessel, allows the dynamic simulation of agitated dispersions, including their response to step and pulse changes in the main process variables, namely, in the flowrates (average residence times), dispersed-phase holdup (phase flow ratio), agitation intensity, dispersed-phase feed drop-size distribution, and continuous- and dispersed-phase feed solute concentrations.

Other details of these models and corresponding algorithms are given elsewhere by Ribeiro et al.[11] This algorithm, further adapted by Regueiras and co-workers[12,13] to model an agitated column, by stagewise solution of the population-balance equa-

* To whom correspondence should be addressed. Tel.: 00-351-234-370733/360. Fax: 00-351-234-3700084. E-mail: CPinto@dq.ua.pt.

[†] Instituto Superior de Engenharia do Porto.

[‡] Faculdade de Engenharia da Universidade do Porto.

[§] Technical University of Munich.

[||] Universidade de Aveiro.

10.1021/ie051453l CCC: $33.50
Published on Web 05/02/2006

Table 1. Physical Properties of Toluene and Water at 20 °C

	density ($kg \cdot m^{-3}$)	viscosity (Pa·s)	interfacial tension ($N \cdot m^{-1}$)
toluene	866.7	0.586×10^{-3}	33.4×10^{-3}
water	998.2	1.003×10^{-3}	

tions under dynamic conditions, was designed to compute the drop-size distribution and local dispersed-phase holdup profiles along the column. Its use yielded an encouraging qualitative agreement with the experimental results obtained in a pilot-plant Kühni column.[6]

By taking into consideration the results of the error analysis performed[6] and their effect, the objective of this paper is to report and discuss the agreement obtained between the simulated and experimental data. Since the hydrodynamics alone was contemplated, all experiments were conducted in the absence of mass transfer, and therefore with no solute, for the purposes of this particular report.

Experimental Work

The experimental work was carried out by Gomes[5] in a Kühni pilot-plant column (150 mm inside diameter, active height of 2520 mm, divided into 36 stirred compartments with 25% free area baffle plates, at the TUM—Technical University of Munich). The test system was the standard equilibrated high interfacial tension toluene (dispersed phase)—water (continuous phase) system. The physical properties of both fluids (at 20 °C) are reported in Table 1.

Experiments at room temperature, under both steady-state and dynamic conditions, were performed under normal and extreme agitation intensity and dispersed- and continuous-phase flow rates. Details of the data reported by Gomes[5] can be obtained from the authors, and other similar data are available from Zamponi.[14]

The extraction column was equipped with measurement devices that allowed the investigation of the hydrodynamic conditions along the column. A photoelectric technique, initially developed by Pilhofer in ref 15, was used to measure the axial drop-size distribution profiles. The drop slug length in a capillary was determined with two pairs of photoelectric cells on a calibrated capillary. This instrumentation was installed in five compartments (2nd, 5th, 11th, 21st, and 35th**)** of the column. Unfortunately, the experimental setup could not provide for the acquisition of the feed drop-size distribution (which was simulated as Gaussian with optimized average and standard deviation) nor even of the drop-size distribution at the first column stage.

Local holdups were monitored at four compartments, namely, the 4th, 10th, 16th, and 22nd, using a noninvasive ultrasonic technique described by Yi and Tavlarides.[16] As a check, the overall column holdup was also measured using the pressure difference between the top and bottom of the active part of the column. All these data, as well as the intensity of agitation and the flow rates of the dispersed and continuous phases, were recorded on-line using a personal computer. Experimental results were obtained as data files created by *Hydromess*, a computer program developed at the University of Clausthal[15] and implemented at the University of Munich's pilot-scale Kühni column. From a collection of 1000-drop size measurements, this program computes number, volume, and surface area drop-size distributions and mean diameters. Drop-size distributions were obtained under steady-state conditions only.

Different runs have been carried out under the same operating conditions but under uncontrolled environmental conditions (in particular, ambient temperature was not measured). Although this could be expected to be an important source of variation of the dispersed-phase size and holdup measured data, no significant difference was observed between measurements in two experimental campaigns at different times of the year.

Several experiments were planned and performed under steady state, and we considered a constant continuous/dispersed-phase flow ratio ($\{Q_C\}/\{Q_D\} = 1.28$). The standard operating conditions were defined for two different sets of fluid flow rates labeled as follows:

B12: $Q_D = 120\ L \cdot h^{-1}$; $Q_C = 94\ L \cdot h^{-1}$; agitation rate = 170 rpm

B16: $Q_D = 160\ L \cdot h^{-1}$; $Q_C = 125\ L.h^{-1}$; agitation rate = 140 rpm

Hydrodynamic Model

This type of column may be approximately described as a sequence of agitated vessels, separated by constricted regions modeled as in intermediate-regime gravitational flow, with dispersed-phase forward and backmixing effects between stages.

The proposed model and parameter optimization algorithm[13] used in the present work combines the drop-interaction model developed by Coulaloglou and Tavlarides[1] with an original phase interstage transport model,[12] and is numerically treated and solved by the same technique developed by Ribeiro et al.[8,9] It was proved capable of describing the hydrodynamic behavior of both the transient and steady state of this type of agitated extractor.

The breakage frequency derived by Coulaloglou and Tavlarides[1] has the following form:

$$g(d) = k_{1Break}\frac{\epsilon^{1/3}}{(1+\phi)d^{2/3}}\exp\left[-k_{2Break}\frac{\sigma(1+\phi)^2}{\rho_D d^{5/3}\epsilon^{2/3}}\right] \quad (1)$$

In the above equation, d is the drop diameter, σ is the interfacial tension, ρ_D is the density of the dispersed phase, ϵ is the energy dissipation per unit mass, and k_{1Break} and k_{2Break} should, in principle, be nearly universal constants.

The daughter drop-size distribution is assumed normal, with mean volume equal to half the volume of the mother drop. It is well-known that the Coulaloglou and Tavlarides breakage frequency expression predicts a maximum, but it has repeatedly been checked that such a predicted maximum occurs for drop sizes much larger than 1 mm, in high interfacial tension systems.

Coalescence frequency is modeled as a product of two factors, the collision frequency, $h(d,d')$, and the coalescence efficiency, $\lambda(d,d')$. To describe the coalescence efficiency, Coulaloglou and Tavlarides have used a probabilistic model, based on the argument that coalescence occurs when the contact time between two colliding drops exceeds the time necessary to drain the liquid film between them to rupture thickness, such that coalescence frequency is

$$c(d,d') = h(d,d')\lambda(d,d'), \quad (2)$$

where the collision frequency is given by

$$h(d,d') = k_{1Coal}\frac{\epsilon^{1/3}}{1+\phi}(d^2 + d'^2)(d^{2/3} + d'^{2/3})^{1/2} \quad (3)$$

and the coalescence efficiency of the collision

$$\lambda(d,d') = \exp\left[-k_{2\text{Coal}}\frac{\rho_C \mu_C \epsilon}{\sigma^2(1+\phi)^3}\left(\frac{dd'}{d+d'}\right)^4\right] \quad (4)$$

where μ_C and ρ_C are the continuous-phase viscosity and density, respectively, and $k_{1\text{Coal}}$ and $k_{2\text{Coal}}$ should also be the nearly universal constants.

It is important to note that the original (but recognizably incorrect) form of the coalescence frequency expression (eq 3) has been used, instead of the correct $(d + d')^2$ first diameter-dependent factor, simply for consistency with all our previous implementations. The only difference is that the $k_{1\text{coal}}$ parameter obtained with the expression used is, as quantitatively expected, approximately twice the correct one, except for very wide drop-size distributions—even wider than those obtained in Kühni column extractors.

These equations reasonably describe the dispersion hydrodynamics within each column compartment, where they may be combined with those describing solute mass transfer between the continuous and dispersed phases, when modeling mass-transfer processes, which was not the case of this particular work. To completely simulate the performance of each compartment, they must also be combined with a transport model describing the interstage flows/velocities of the continuous-phase and dispersed-phase drops.

From the mathematical model,[9] the drop birth and death rates due to breakup, coalescence, and drop movement along the column are calculated. Representing these source and sink terms by $B(\bar{n},t)$ and $D(\bar{n},t)$, at time t and location $[\bar{n}, \bar{n} + d\bar{n}]$ of the drop phase space, the dynamics of the drop number density function $X(\bar{n},t)$ may be described by

$$\frac{\partial}{\partial t}X(\bar{n},t) + \frac{\partial}{\partial \bar{n}}\left[\frac{\partial \bar{n}}{\partial t}X(\bar{n},t)\right] = B(\bar{n},t) - D(\bar{n},t) \quad (5)$$

To numerically solve the above population-balance equation, a phase space-time discretization is used and drops are assumed to reside on cell sites. Drops move from cell to cell in the discretized phase-space at each time step. The numerical integration scheme involves the explicit calculation of time derivatives, with a first-order backward finite-difference method.[9]

The transport model has been developed[12] based on a previous one described and used by Cruz-Pinto.[2] Some concepts will be described here in some detail.

Whatever model is chosen to describe column hydrodynamics, single-drop terminal velocities must be considered when calculating slip velocities. For countercurrent flow, the slip velocity is equal to the sum of the superficial velocities of the phases in the dispersion. The slip velocity[17] of the dispersion is defined as the sum of the ratio of volumetric throughput and the cross section accessible for the flow of the phase considered. The resulting equation is

$$v_{\text{slip}} = \frac{V_D}{\phi} + \frac{V_C}{1-\phi} \quad (6)$$

It is, however, still necessary to allow for the effect of the column internals on slip velocity by using a constriction factor, C_R, as follows

$$v_{\text{slip}} = \frac{1}{C_R}\left(\frac{V_D}{\phi} + \frac{V_C}{1-\phi}\right) \quad (7)$$

It is useful to compare single-drop terminal velocities with velocities of rigid spheres under otherwise identical conditions. As considered by Mišek,[18] the drops may (1) depart from spherical shape, (2) develop internal circulation, (3) oscilate and vibrate, and (4) split. The three first types of behavior cause the deviation of terminal drop velocities from those of rigid spheres; the fourth type changes the situation entirely.

In an agitated dispersion, the deviation from spherical shape and oscillation and vibration have a random character. Concerning the vertical component of single-drop velocity, the conditions within an agitated liquid−liquid dispersion may be closer to the rigid drop velocity than in other cases. The terminal velocity, v_T, of rigid spheres has been correlated, allowing for the dispersion density and drag coefficient effects.[2]

In the region of small drop sizes and small drop Reynolds numbers, not applicable to an agitated column, the dependence corresponds to Stokes' law

$$v_T = \frac{g\Delta\rho d^2}{18\mu_C} \quad (8)$$

To describe the useful intermediate law, which is typical of a Kühni liquid−liquid extraction column,

$$v_T = 0.249d\left[\frac{g^2\Delta\rho^2}{\rho_C\mu_C}\right]^{1/3} \quad (9)$$

where $\Delta\rho = (1-\phi)(\rho_C - \rho_D)$ and ρ_C and μ_C are the density and the viscosity of the continuous phase, respectively. The vertical movement of drops in the region of very high Reynolds numbers departs drastically from rigid drop behavior. In this region, the extractor operation is not very typical.

The usual countercurrent movement of the dispersed and continuous phases differs significantly from the movement of individual droplets. The droplets influence each other in their behavior, either directly or by means of the continuous phase. The final effect is complicated.

The drop dispersion effect was modeled by means of a random disturbance on the terminal drop velocities (because of the agitation intensity), as a function of the rotor peripheral velocity. The constriction factor, C_R , which controls the drop passage between stages, was calculated based on a linear expression suggested by Goldmann,[19] as a function of the fractional free area of the stage separators.

$$C_R = (1 - k_{1\text{Transport}})e + k_{1\text{Transport}} \quad (10)$$

where e is the fractional free area and $k_{1\text{Transport}}$ is a transport parameter for the effective flow area in interstage constrictions.

The random component of the drop velocity is assumed to be isotropic and to have an average magnitude described by Regueiras and co-workers[12,13] as a fraction of the velocity of the impeller tip

$$v_D = k_{2\text{Transport}}ND_R\pi \quad (11)$$

where v_D is a radial velocity of the continuous phase, $k_{2\text{Transport}}$ is a transport parameter for modeling the size-dependent axial dispersion (i.e., the effect of a random variation of the drop velocities), N is the rotor speed, and D_R is a rotor diameter.

The axial slip velocity (drop velocity relative to the continuous phase) in each size class is then modified by summing or subtracting the average value of the axial projection of this random component, and the number fraction of drops of each class that pass from one compartment to each of its neighbors is computed accordingly. This approach is merely a more-general formulation of the axial dispersion than the one suggested by Tsouris.[20]

The correlations used (in the most recent simulations) to calculate the power input rate as a function of the rotor's angular velocity were those developed by Kumar and Hartland,[21] in their effort to find unified correlations for some of the most common agitated liquid−liquid extraction columns, which are claimed to describe reasonably well the experimental results.

Here, for the calculation of the agitation speed-power density, the correlation used is given by

$$\epsilon = \frac{4P(k_{1\text{PowerFact}})^3}{\pi {D_C}^2 H[\rho_C(1-\phi)+\rho_D\phi]} \tag{12}$$

where $k_{1\text{PowerFact}}$ is a parameter for the agitation speed-power density, ρ_C and ρ_D are the density of the continuous and dispersed phases, respectively, ϕ is the dispersion phase holdup, P is the power input per compartment, H is the compartment height, and D_C is the internal column diameter.

The power input, P, to each column compartment is

$$P = N_P {N_I}^3 {D_R}^5 \rho_C \tag{13}$$

The power number, N_P, is given by the correlation obtained by Fischer in ref 21,

$$N_P = 1.08 + \frac{10.94}{{Re_R}^{0.5}} + \frac{257.37}{{Re_R}^{1.5}} \tag{14}$$

with $Re_R = N_I {D_R}^2 \rho_C/\mu_C$, where D_R is the agitator diameter and N_I is the agitation rate.

In the absence of direct experimental measurements at the dispersed-phase distributor outlet, an average value (inMeanDiamD) and a standard deviation (inStdDiamD) of the feed drop diameter distribution have been considered, which were iteratively adjusted[5] together with the seven intrinsic model parameters. The feed drop diameter distribution is assumed to be log-normal. In fact, preliminary runs have shown that, among various distribution types, this is the most adequate to describe our data.

The performance of this algorithm in describing the hydrodynamics of the Kühni column was presented and discussed, in its first implementation, by Regueiras et al.[12] In that work, a first attempt has been made at a qualitative adjustment of the simulation to the experimental results, which highlighted the potentialities of the model and its broad adequacy for the purpose. The model, however, given its physical and mathematical complexity, involves up to nine parameters, which will have to be determined and/or adjusted in any quantitative description of the experimental behavior.

The optimization algorithm selected was Levenberg−Marquardt's, for its recognized capability of handling highly multidimensional spaces and its economy on function calls, in cases where the objective function deviates significantly, even close to a minimum, from a quadratic behavior—the ideal for second-order methods. The objective function was defined as a weighed sum of the squared deviations between calculated and experimental values of the overall and local dispersed-phase holdups and of the local cumulative, number-based, drop-size distributions, as follows

$$1 \times (\phi - \overline{\phi})^2 + \frac{1}{4} \times \sum_i (\phi_i - \overline{\phi_i})^2 + \frac{1}{80} \times \sum_j \sum_k (c_{j,k} - \overline{c_{j,k}})^2 \tag{15}$$

where $i = 1, ..., 4$ is the holdup sampled compartment number; $j = 1, ..., 5$ is the size distribution sampled compartment number; and $k = 1, ..., 16$ is the cumulative size distribution (c) class number.

Table 2. Drop Interaction Parameter Values of Bapat[25]

$k_{1\text{Break}}$	$k_{2\text{Break}}$	$k_{1\text{Coal}}$ (cm^{-3})	$k_{2\text{Coal}}$ (cm^{-2})
0.00481	0.0800	0.001	2×10^8

The implementation adopted was that due to Nash[22] and written by Regueiras;[13] it uses double precision (64 bits: 1 for sign, 11 for exponent, 52 for the mantissa; range $\pm 1.7 \times 10^{308}$ with at least 15 digits of precision) in all critical number representations, and it is especially careful in the estimate of the objective function derivatives. Separate reports will more fully describe and discuss these computations and their results.

The algorithm was implemented in C++, and the corresponding program has a friendly Windows interface for data entry.[13,23] In the interface, the user may choose

- Column description (number of stages, internal diameter, stage height, stirrer diameter, and open free area);
- Numeric models (breakage and coalescence, and transport parameters);
- Values of the physical parameters of the liquid−liquid system under study (specific gravity, viscosity, and interfacial tension);
- Experimental operating conditions (flow rates of the dispersed and continuous phases, stirrer speed, and drop-size distribution); and
- Drop class grid (min diameter, max diameter, and number of logarithmic classes, to ensure uniform relative precision in drop sizes).

The program begins at time $t = 0$, where the column variables are initialized to a standard initial state, corresponding to a column filled with continuous phase and no dispersed phase, similar to the real experimental run conditions. The description of the sequential algorithm and the corresponding flowchart may be found in the work of one of our collaborators,[24] which also considered its parallelization, for greatly improved performance.

To validate the model and the corresponding algorithm, several simulation runs were carried out, using phase flows, agitation intensities, and start-up conditions identical to those of the actual pilot-plant experiments. The parameter values used in other drop population balances by the same team,[25] often claimed to be nearly universal constants for agitated liquid−liquid contactors, were also adopted here (Table 2).

Optimization Procedure—Preliminary Systematic Parameter Search

With the double objective of transferring the physical knowledge gained in our operation of TUM's pilot-plant column[5] to the manipulation of the model parameters and to obtain a first plausible approximation to their values (to be later used as the starting point in the Levenberg−Marquardt optimizations), a preliminary search was performed, within a reasonable range of values.

The target values for the local and overall dispersed-phase holdup and for the number-based drop-size distributions were tested against the confidence interval calculated from the actual experiments.[6] Following the experiment-based indication by Zamponi[14] that the agitation intensity stands out as the most sensitive operating variable, the simulations concentrated initially on the prediction of the steady state of experiments with two given sets of continuous- and dispersed-phase flows (standard operating conditions B12 and B16).

Table 3. Values of the Operating Conditions and Interaction and Transport Model Parameters Used

simulation 1	simulation 2
$k_{1Break} = 0.004\ 81$	$k_{1Break} = 0.004\ 81$
$k_{2Break} = 0.08$	$k_{2Break} = 0.08$
$k_{1Coal} = 0.001$	$k_{1Coal} = 0.001$
$k_{2Coal} = 2 \times 10^8$	$k_{2Coal} = 2 \times 10^8$
$k_{1Transport} = 1$ (inMeanDiamD = 0.24)	$k_{1Transport} = 1$ (inMeanDiamD = 0.24)
$k_{2Transport} = 0.2$ (inStdDiamD = 0.048)	$k_{2Transport} = 0.6$ (inStdDiamD = 0.048)
$k_{1PowerFact} = 1$	$k_{1PowerFact} = 1$

Various sets of runs were made with the drop-interaction parameters values given in Table 2 and the three parameter values considered for the transport model. From the results obtained, the search entered a new phase, in which first the drop-interaction model parameters and then the transport model parameters were varied. This first semiquantitative adjustment is presented in Gomes,[5] where the predicted results are compared with the experimental ones, showing the various steps followed.

This preliminary adjustment of the model parameters is essential, whenever the convexity of the objective function is not guaranteed, with the possibility of reaching spurious or local minima. Number-based drop-size distributions were used in the definition of the objective function.

Results and Discussion

In the preliminary systematic parameter search, the simulations concentrated initially on the prediction of the steady state of experiments with two given sets of continuous- and dispersed-phase flows (standard operating conditions B12 and B16).

(i) When using the drop-interaction parameter values given in Table 2, together with arbitrary values for the transport model parameters, it was first observed that both local and overall simulated dispersed-phase holdups were too high. The drop-size distribution's variation was different from that of the experiments, namely, for low agitation, the distributions at the second stage were shifted to larger drop sizes, and at increasing column heights, the distributions strongly shifted to much smaller drop sizes, corresponding to excessively high breakage frequencies relative to those apparently prevailing in the experiments. When working in the standard operating conditions B16, the distribution obtained for the second stage resembled the experimental one, but at the fifth stage, a completely different, right-tailed distribution was predicted.

(ii) From these results, the search entered a new phase, in which first the drop-interaction model parameters and then the transport model parameters were varied. From the close study of the results, we could conclude that the transport model needed correction, such as to include eq 10 for the C_R factor and eq 14 for the power number. The expression for the power number was then kept unchanged in all simulations. We also concluded that the dispersed-phase feed drop-size distribution also needed adjustment (through the average and standard deviation of its log-normal distribution), as a function of the operating conditions, instead of being treated as constant.

(iii) The ensuing computer simulations were performed without changing the drop breakage (k_{1Break} and k_{2Break}) and coalescence (k_{1Coal} and k_{2Coal}) parameters, by adjusting the axial dispersion parameter, $k_{2Transport}$ (eq 11), and the characteristics of the drop feed size distribution—a total of 3 effectively variable parameters.

Considering large values for drop size in the feed and a given axial dispersion parameter (cf. Table 3), the distribution shifts to smaller drop sizes right from the second stage, and coalescence shows its presence mainly in the upper stages of the column. Also, the resulting dispersed-phase holdups decrease. If one considers a large-drop-size dispersed-phase feed and $k_{2Transport}$ is increased (cf. Table 3), the number distribution in the second stage shifts to smaller drop sizes, as shown in Figure 1, and the overall holdup value decreases.[5]

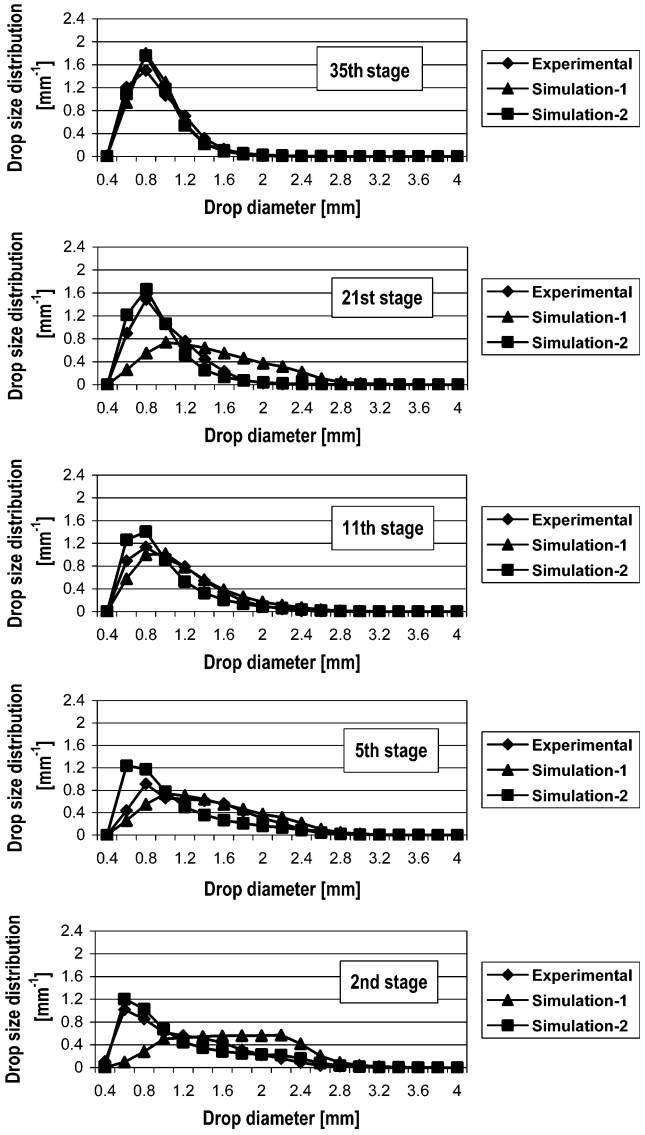

Figure 1. Drop-size number distributions under operating conditions B16-standard ($Q_C = 125$ L·h^{-1}; $Q_D = 160$ L·h^{-1}; 140 rpm).

One thing is thus made clear: an increased dispersion effect brings the simulated results closer to the experimental ones, while a less intensive dispersion appears to favor coalescence at the lowest stages, excessively broadening the distributions. Table 3 shows the input data used in the simulations that yielded the results of Figure 1.The parameters used in these simulations correspond to the conditions of Simulations 1 and 2 shown in Table 3.

Runs were also carried out with unchanging $k_{2Transport}$ and inMeanDiam but variable inStdDiam. What was found was that, when the standard deviation is lowered to half, the dispersed-phase holdups slightly increase and increased numbers of larger drops appear in the second stage but, in general, the shape of the size distributions does not significantly change. On the other hand, when the standard deviation is doubled, increased numbers of smaller drops result in the lower stages of the column.

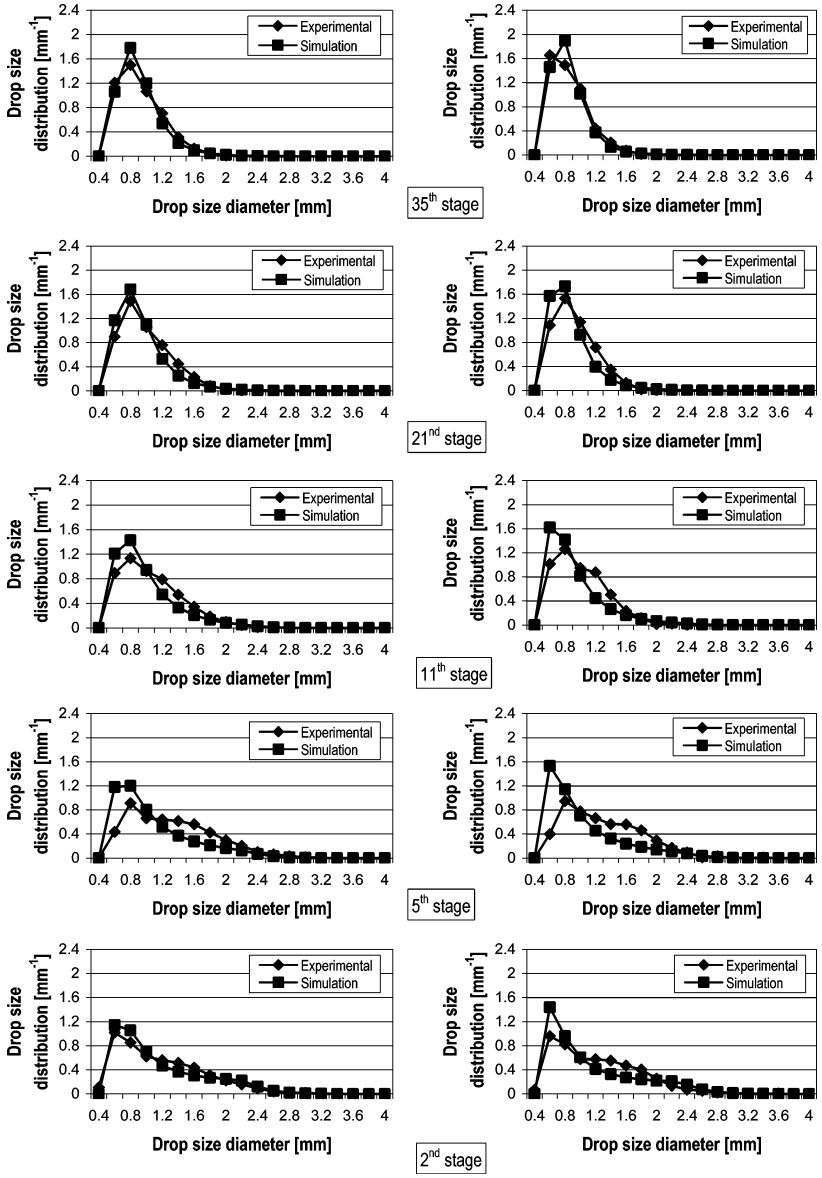

Figure 2. Simulated and experimental values of drop-size number distribution profiles under operating conditions B16 ($Q_C = 125$ L·h^{-1}; $Q_D = 160$ L·h^{-1}): (left), 140 rpm; (right), 150 rpm.

Figure 2 presents the local (experimental and simulated) drop-size distributions, for two different agitation intensities under operating conditions B16. The agreement obtained demonstrates that the model is capable of reasonably describing the dispersed-phase behavior stage by stage. The parameters used in these simulations correspond to the conditions of Simulation 2 shown in Table 3.

It is worth mentioning again that these experimental and computer runs correspond to ordinarily used agitation intensities. When the agitation is lowered to 100 rpm, keeping the feed's characteristics unchanged, varying the dispersion parameter does not change the shape of the predicted drop-size distributions. At these conditions, to obtain distributions closer to the experimental ones, the drop-breakage parameters must be changed, as will be shown next. Changing the coalescence parameters, however, does not significantly improve the predicted results.

The confidence channel for local drop-size distributions, calculated from the student's *t*-distribution[6] for six runs under standard operating conditions B12, were compared with the corresponding simulated results using two different sets of values for the drop-interaction parameters.

Table 4. Drop Interaction Parameters of Bapat,[25] with Small Modifications on the Breakage Parameters, and Remaining Model Parameters Used in the Simulation of the Results of Figure 3

simulation ($N_I = 100$ rpm)	simulation ($N_I = 140$ rpm)
$k_{1Break} = 0.003\,6$	$k_{1Break} = 0.003\,6$
$k_{2Break} = 0.1$	$k_{2Break} = 0.1$
$k_{1Coal} = 0.001$	$k_{1Coal} = 0.001$
$k_{2Coal} = 2 \times 10^8$	$k_{2Coal} = 2 \times 10^8$
$k_{1Transport} = 0.25$ (inMeanDiamD = 0.18)	$k_{1Transport} = 0.25$ (MeanDiamD = 0.18)
$k_{2Transport} = 1$ (inStdDiamD = 0.042)	$k_{2Transport} = 1$ (inStdDiamD = 0.036)
$k_{3Transport} = 0$	$k_{3Transport} = 0$
$k_{1PowerFact} = 1$	$k_{1PowerFact} = 1$

As may be seen in Figure 3, the deviation of the predicted from the experimental distributions does not fall significantly outside the confidence limits. The worst agreement obtained for the fifth stage, as illustrated on the left of Figure 3, is possibly due to the drop-size measurement probe problems and errors incurred at this particular column location, when using Bapat's breakage and coalescence parameters without modifica-

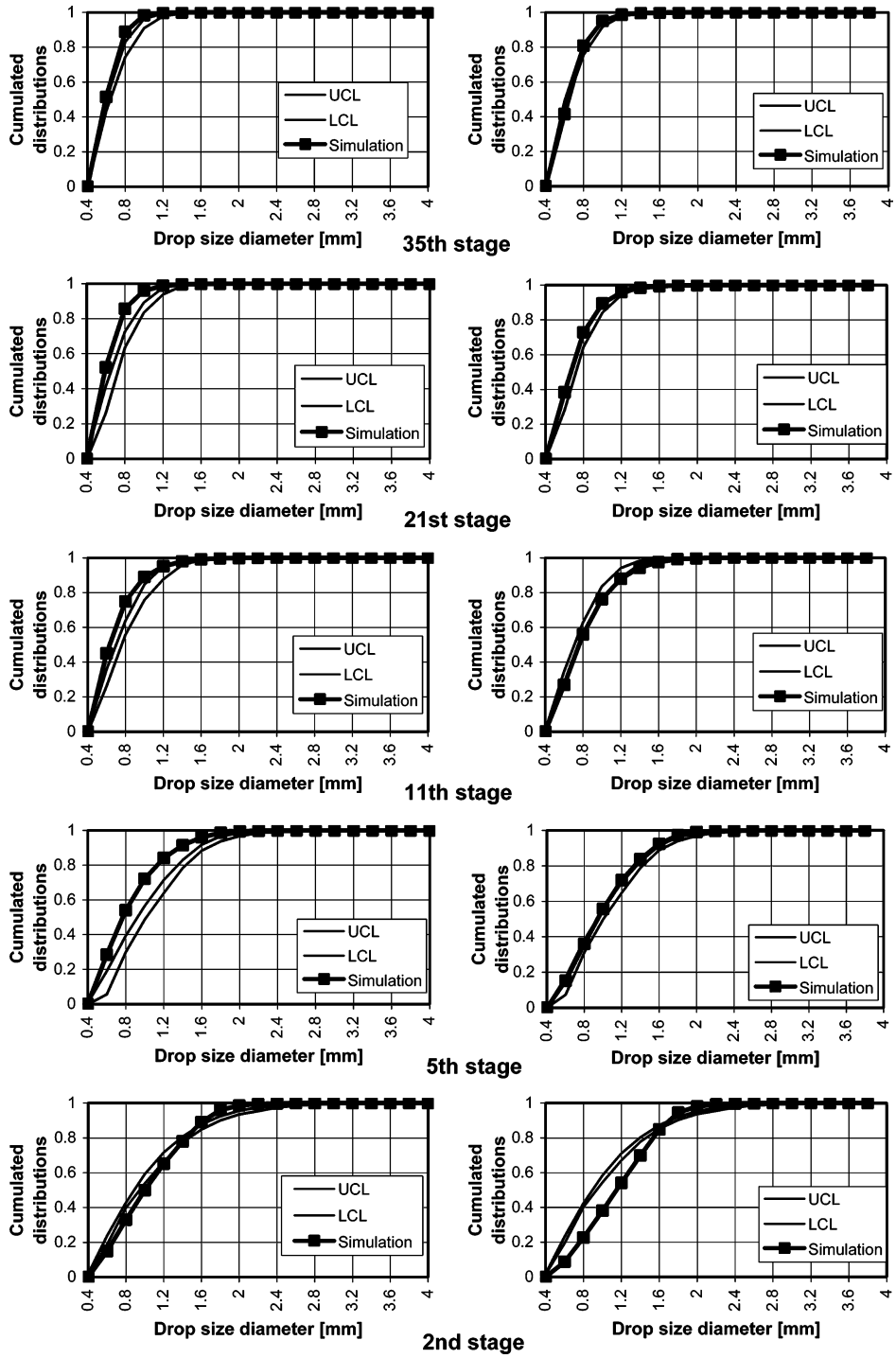

Figure 3. Simulated values of drop-size distributions, together with confidence limits. Standard operating conditions B12 ($Q_C = 94$ L·h^{-1}; $Q_D = 120$ L·h^{-1}; 170 rpm): (left) Simulation with Bapat's parameters; (right) Simulation with variations on Bapat's parameters; UCL = upper (98%) confidence limit; LCL = lower (98%) confidence limit.

tion. The values obtained for the dispersed-phase holdup are also excessive, 30% higher than the measured ones.

However, a relatively small (ca. 20%) change in the breakage parameters relative to the original Bapat's values of Table 2 (as shown in Table 4) yields the results shown on the right side of Figure 3. In this case, the worst agreement is now obtained at the lowest stage, which may reasonably be attributed to the lack of any direct data on the dispersed-phase feed drop-size distribution, with the available column instrumentation.

Figure 4 shows the local number-based (experimental and simulated) drop-size distributions for normal (140 rpm) and low (100 rpm) agitation column operating conditions. The breakage, coalescence, and transport model parameter values used in these simulations are those given in Table 4 and, thus, include adjustments on Bapat's breakage parameters and on the transport and dispersed-phase feed distribution parameters.

One may notice that the bimodal character of the experimental drop-size distributions is indeed predicted by the models. Most important, for the lowest agitation intensity, a marked coalescence effect is detected,[26] even at the highest column stages. It is also observed that, while at 140 rpm the agreement is very reasonable, at 100 rpm it becomes clearly worse, with the highest deviations being obtained for the lowest instrumented column stage (the second), closest to the dispersed-phase distributor, at

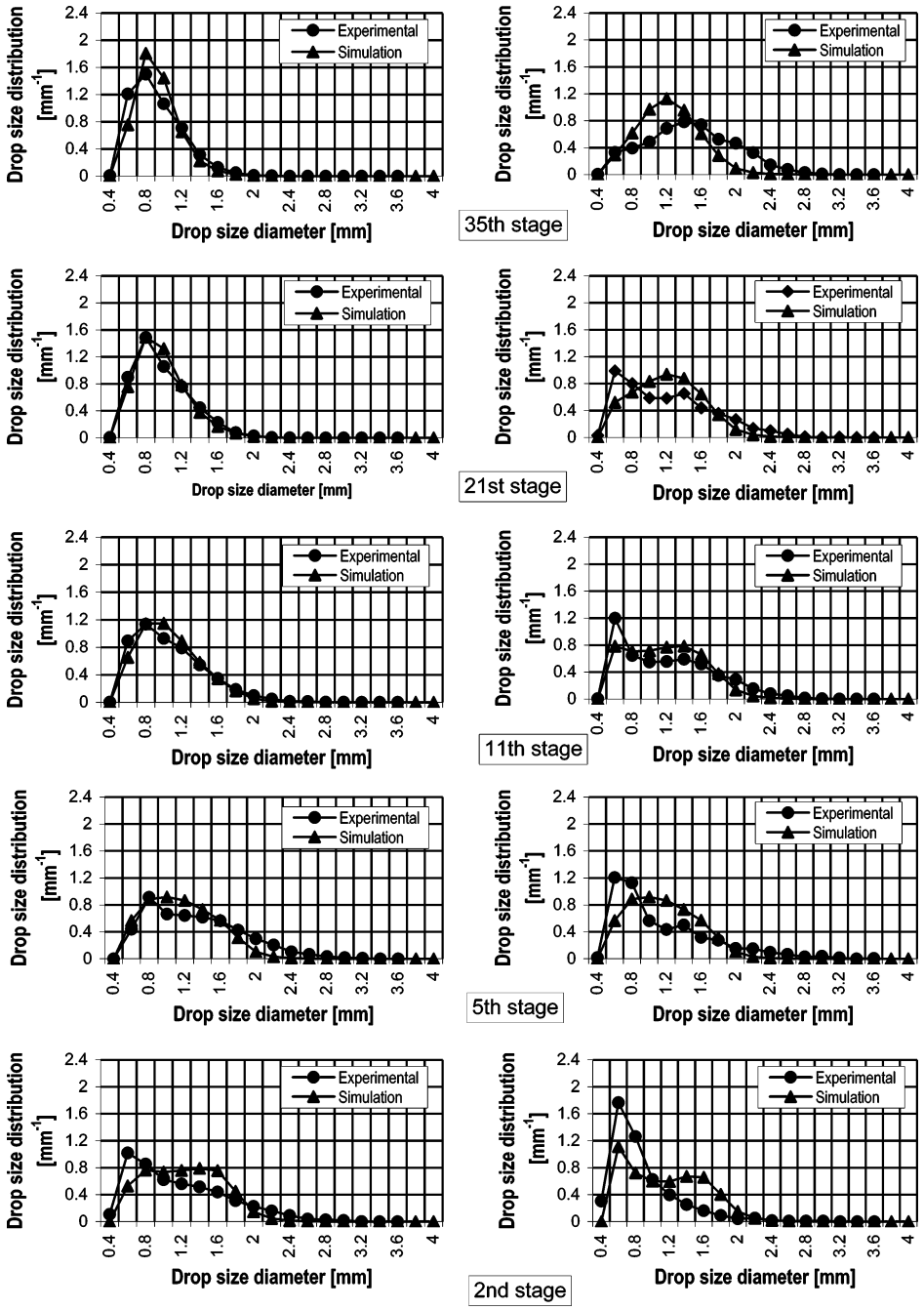

Figure 4. Simulated and experimental values of drop-size number distributions at the different stages of the column under operating conditions B16 (Q_C = 125 L·h^{-1}; Q_D = 160 L·h^{-1}): (left), 140 rpm; (right), 100 rpm.

which the dispersed-phase (feed) drop-size distribution had to be estimated, because of lack of instrumentation.

The agreement obtained for the local dispersed-phase holdup values is within the errors calculated from the repeat experimental runs and may, thus, be considered satisfactory, especially if we consider that these simulations have not yet been optimized. These initial (unoptimized) local holdup profiles are shown in Figure 5.

At this point, the reasonable (as yet unoptimized) agreement obtained between the simulated and the experimental results for the pilot Kühni column suggested that Coulaloglou and Tavlarides's drop-interaction model and the population-balance algorithms used may be appropriate to describe the dispersed-phase behavior in agitated liquid−liquid extraction columns, such as the one used in this work, and that probably only not-too-significant changes are still needed on some of their

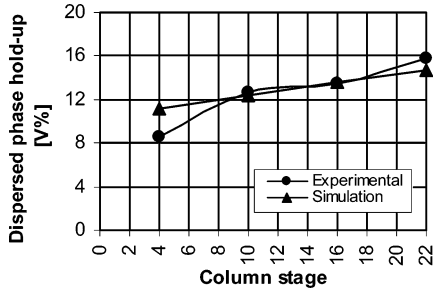

Figure 5. Local dispersed-phase holdup profiles under standard operating conditions B16 (Q_C = 125 L·h^{-1}; Q_D = 160 L·h^{-1}; 140 rpm).

breakage and coalescence parameters, as applicable to simple agitated vessels.[7] If fully validated, this may be of significant theoretical and practical importance.

Table 5. Comparison of the Optimized Parameters with the Preliminary Estimates

parameters	preliminary adjustments	optimized parameters
InMeanDiamD	0.18	0.207 053
InStdDiamD	0.03 6	0.050 769
DropDistribution	LogNormal	LogNormal
k_{1Break}	0.003 6	0.002 991 550
k_{2Break}	0.1	0.897 130
k_{1Coal}	0.001	2.312 980
k_{2Coal}	200 000 000	161 740 000
$k_{1Transport}$	0.25	0.309 618
$k_{2Transport}$	0	0.581 431
$k_{1PowerFact}$	1	2.702 1
SumSquares	0.007 700 00	0.001 505 93

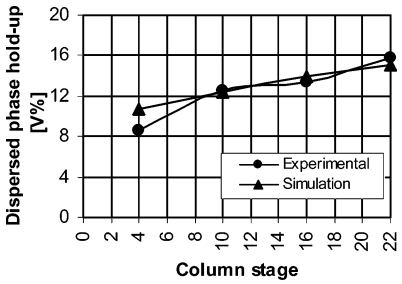

Figure 7. Local dispersed-phase holdup profiles under standard operating conditions B16 with new parameter values.

The right side of Table 4 presents the final model parameter values, which were then (after this preliminary search) used as our initial guesses, in the full numerical parameter optimization computations, for a log-normal feed drop-size distribution.

Because of the excessive computation time spent in each optimization, only in one situation an overall parameter optimization was performed—the average run,[5] under standard operating conditions B16. Even so, the final computer run took more than 3 months of processor time on the fastest microcomputer that we had available.

Having dealt with these difficulties, we then tried to adjust the transport and dispersed-phase feed parameters, keeping the

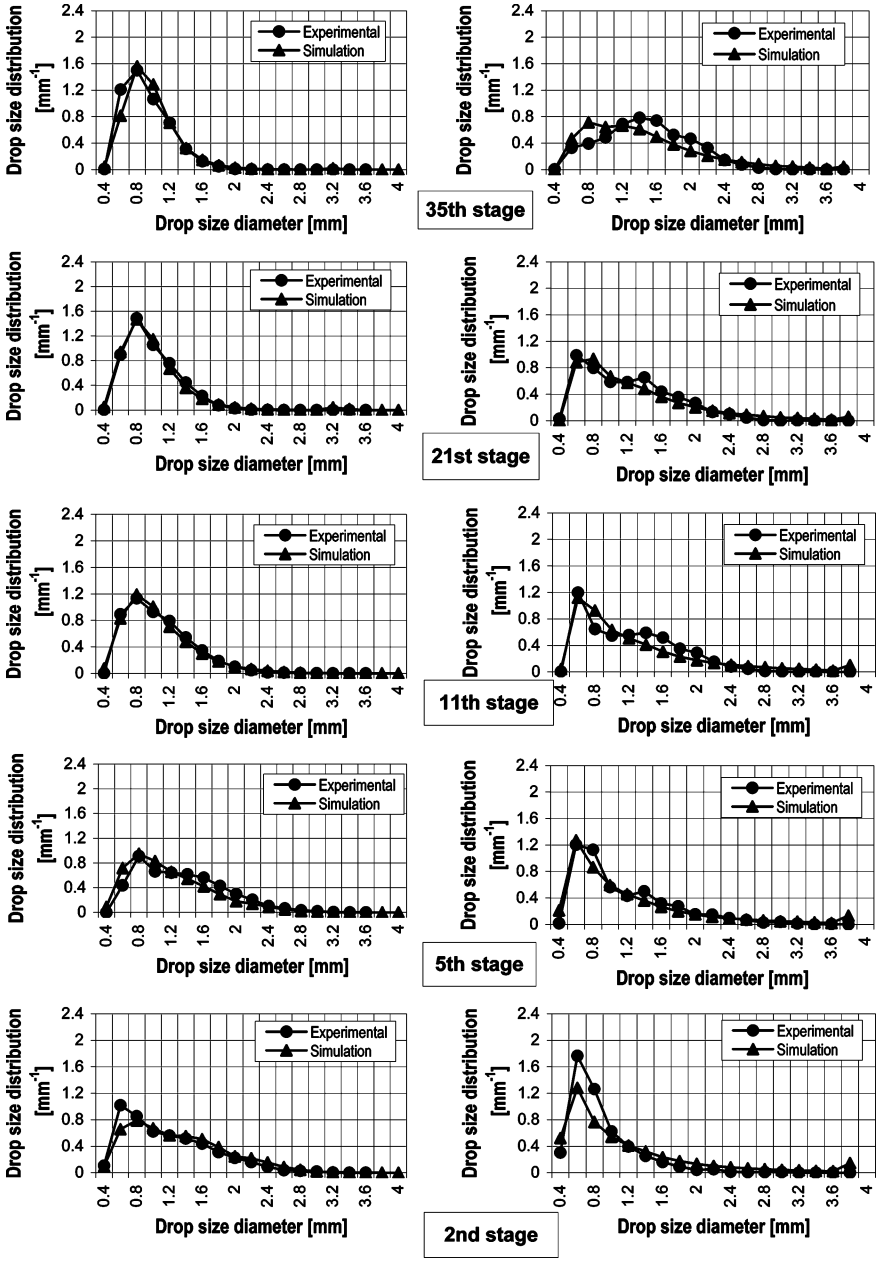

Figure 6. Simulated and experimental values of drop-size number distributions under operating conditions B16 ($Q_C = 125$ L·h^{-1}; $Q_D = 160$ L·h^{-1}): (left), 140 rpm; (right), 100 rpm with new parameter values.

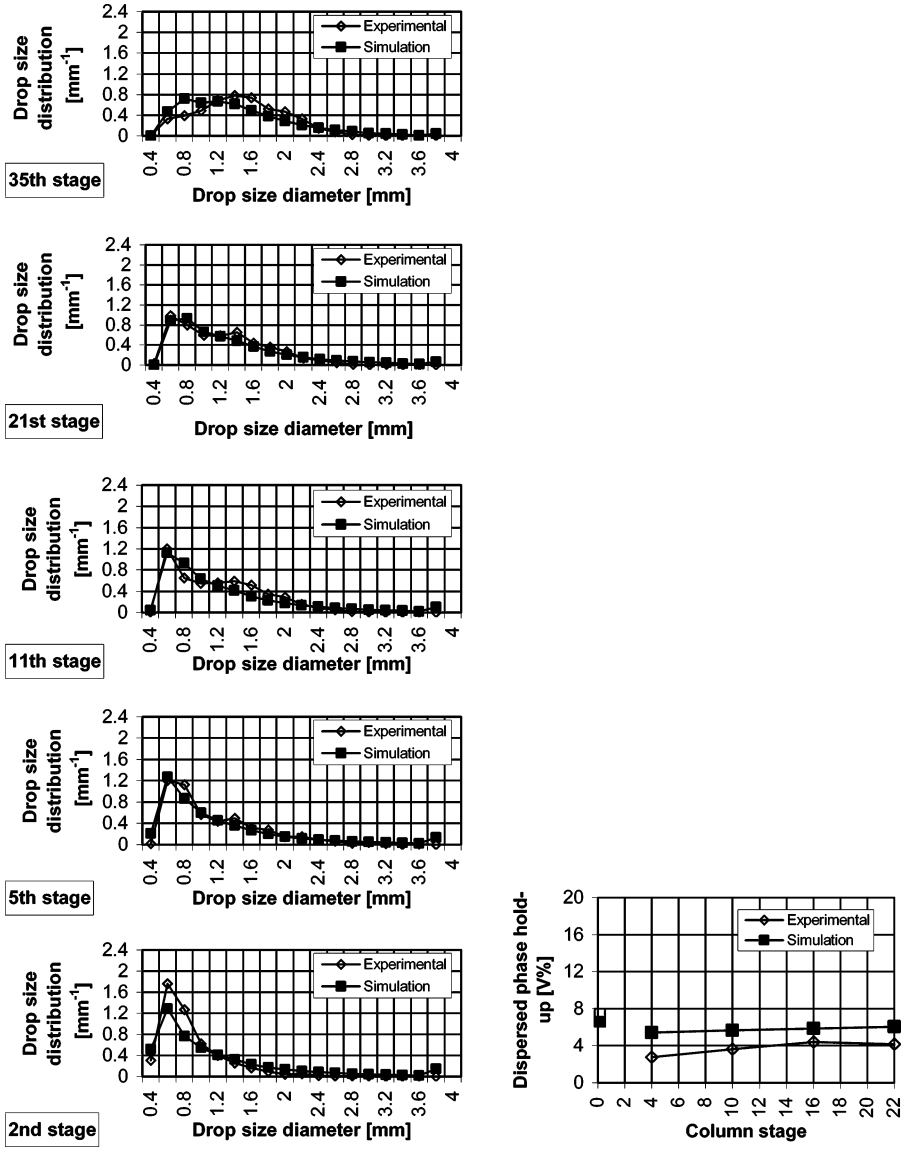

Figure 8. Simulated and experimental values for operating conditions $Q_C = 125$ L·h^{-1}, $Q_D = 160$ L·h^{-1}, and 100 rpm: (left), drop-size number distributions, Run A1 (Table 7); (right), local dispersed-phase holdup profiles, Run A1 (the overall dispersed-phase holdup is represented as that of stage 0).

Table 6. Results of Extrapolating the Model Parameters to New Operating Conditions

run	modified condition	SumSquares
A1	rpm = 100	0.068 019 9
A2	rpm = 120	0.021 687 8
A0	rpm = 140	0.001 505 93
A3	rpm = 150	0.004 720 05
A4	$Q_C = 112.5$	0.001 579 75
A0	$Q_C = 125$	0.001 505 93
A5	$Q_C = 137.5$	0.002 368 05
A6	$Q_D = 144$	0.001 980 71
A0	$Q_D = 160$	0.001 505 93
A7	$Q_D = 176$	0.002 024 21

drop interaction parameters unchanged; the resulting improvement of the simulated results were not encouraging. The results improved significantly only after we decided to free the drop-interaction parameters and the power factor. Significant reductions in the objective function were then achieved, together with a much-improved agreement of the simulated and experimental drop-size distributions.

The (optimized) parameter values obtained are given in Table 5, where they may also be compared with the preliminary estimates. The quality of the new fits, not very easy to evaluate from the objective function values (which, nonetheless, are about 5 times lower than those with the initial parameter estimates), may be better appreciated by comparison of Figures 4 and 6. For the holdup values, the difference is less significant (Figures 5 and 7). Except for the local dispersed-phase holdup at the fourth stage (probe closer to the distributor), the quality of the fits may be considered excellent.

This clear improvement of the fit of the simulated to the experimental results, having been obtained after not-insignificant changes to some of Coulaloglou-Tavlarides's model parameters used by Bapat (particularly, k_{1Coal}), deserves a few comments:

(a) The need for opposite variations in both coalescence parameters, which mutually amplify their effect on the coalescence frequencies, clearly shows the need to predict much higher values of the coalescence frequencies in a Kühni column. This is a major finding, providing a theoretical modeling background for the experimental observations.[5]

(b) The need for an increased power factor, in combination with the above coalescence-parameter variations, thus also significantly increasing the drop-breakage frequencies relative to the coalescence ones, may highlight the possible weakness, not necessarily of Coulaloglou and Tavlarides's interaction model, but of the initially assumed, unoptimized, parameter

Table 7. Dispersed-Phase Feed Distribution Fits to New Operating Conditions

					SumSquares	
run	modified condition	InMean DiamD	InStd DiamD	$k_{1\text{Transport}}$	before	after
A1	rpm = 100	0.081 779 5	0.363 135 9	0.500 706	0.068 019 9	0.003 292 98
A2	rpm = 120	0.141 447 9	0.112 166 7	0.374 894	0.021 687 8	0.001 720 72
A0	rpm = 140	0.207 053	0.050 769	0.309 618	0.001 505 93	
A3	rpm = 150	0.200 632 9	0.005 224 3	0.339 206	0.004 720 05	0.003 396 64
A4	Q_C = 112.5	0.206 100	0.055 982 5		0.001 579 75	0.001 569 33
A0	Q_C = 125	0.207 053	0.050 769		0.001 505 93	
A5	Q_C = 137.5	0.202 945	0.042 520 7		0.002 368 06	0.002 302 23
A6	Q_D = 144	0.195 632	0.045 850 0		0.001 980 71	0.001 837 87
A0	Q_D = 160	0.207 053	0.050 769		0.001 505 93	
A7	Q_D = 176	0.202 136	0.036 108 3		0.002 024 21	0.001 831 93

values and perhaps also of the assumed agitation power correlation (arbitrarily kept unchanged) to cylindrically cross-sectional, completely full, unbaffled, continuous-flow agitated vessels, despite their author's claims on their soundness and broad applicability. Additionally, and most importantly, it clearly points to a possible physical (and, therefore, mathematical) correlation between coalescence and breakage frequencies, yet to unravel and, hopefully, model. However, one should underline that, though with some unexpectedly different parameter values (relative to previously published but unoptimized data), the drop-interaction model itself correctly predicts all effects observed in the experimental steady-state behavior, a feature that many authors have not so far been inclined to accept but which these results document. One should, therefore, consider that the model essentially accounts for the correct phenomenology. However, it is still wise to suggest keeping this problem under study, to clarify all the above physical and modeling problems.

A drastic test of the model's robustness is the parameter's extrapolability to entirely different operating conditions (standard operating conditions B16−A_0), at steady-state conditions. The

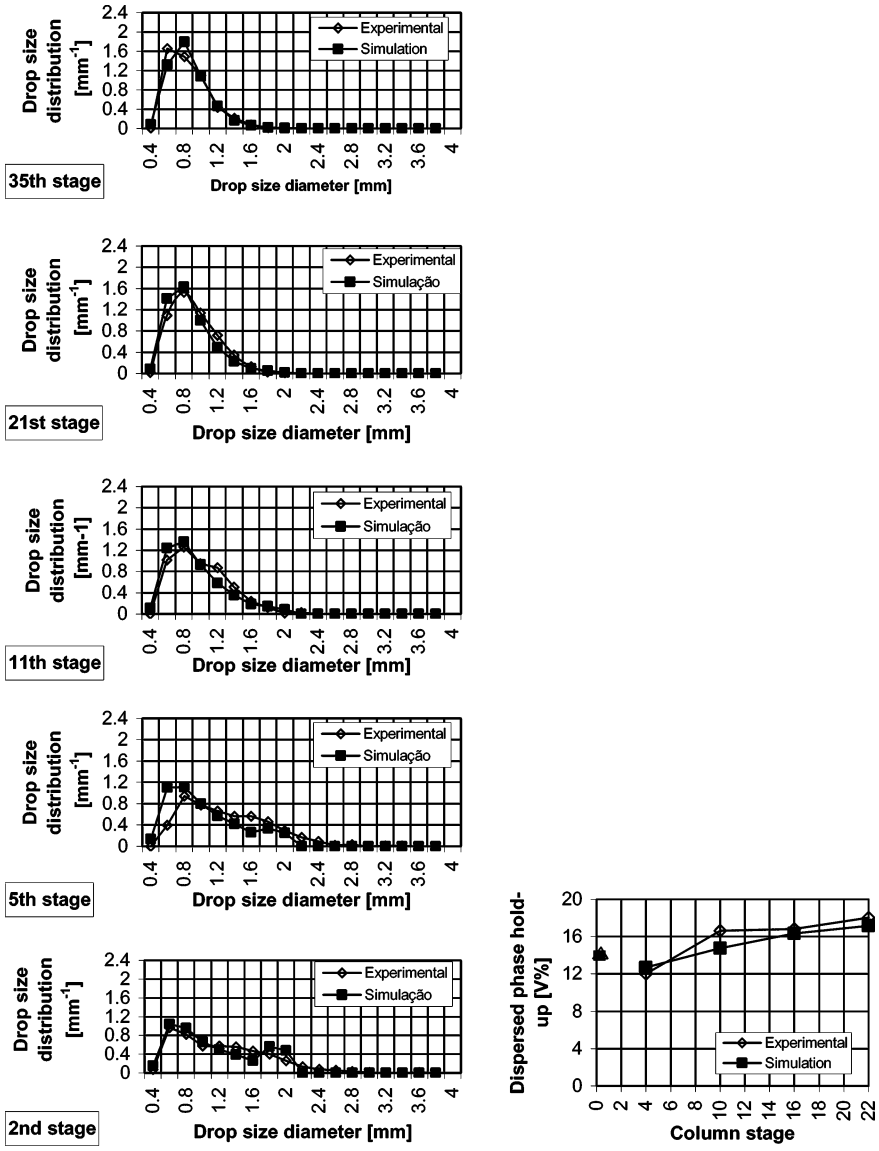

Figure 9. Simulated and experimental values under operating conditions Q_C = 125 L·h^{-1}, Q_D = 160 L·h^{-1}, and 150 rpm: (left), drop-size number distributions, Run A3 (Table 7); (right), local dispersed-phase holdup profiles, Run A3 (the overall dispersed-phase holdup is represented as that of stage 0).

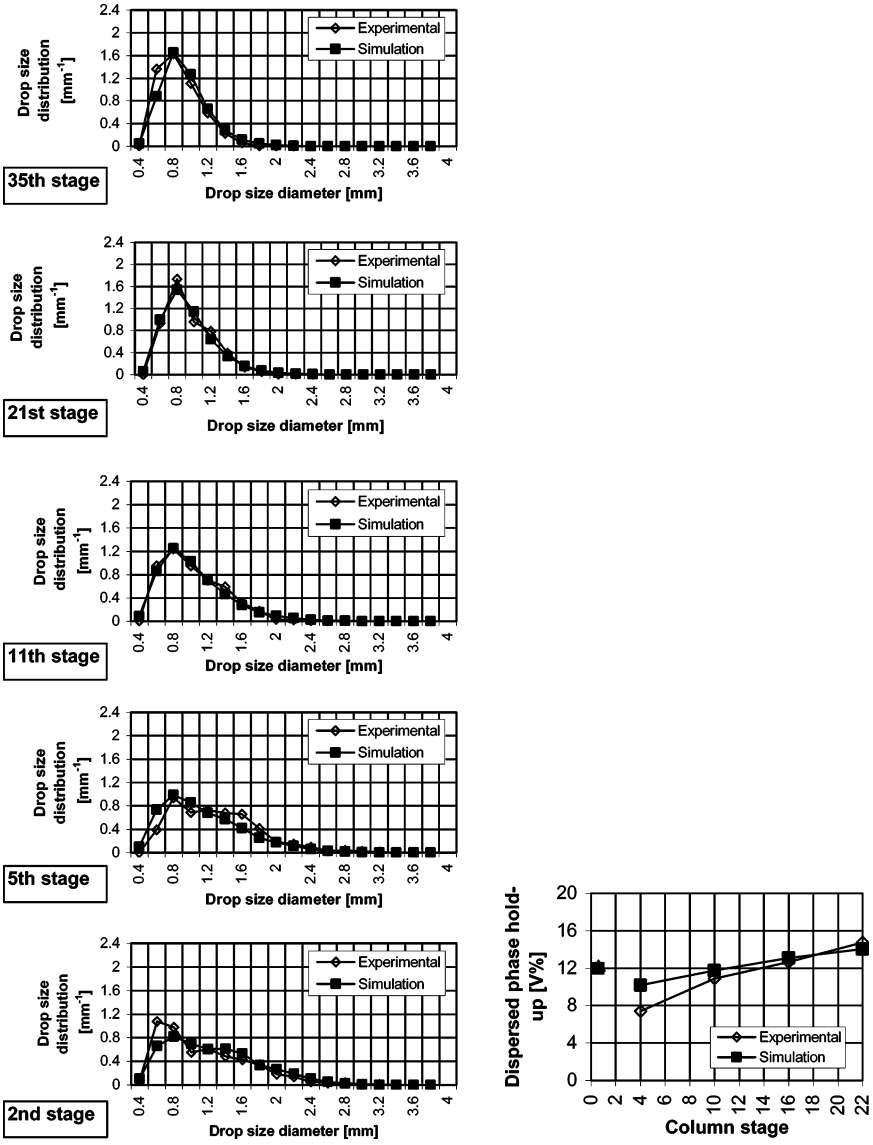

Figure 10. Simulated and experimental values under operating conditions $Q_C = 125$ L·h^{-1}, $Q_D = 144$ L·h^{-1}, and 140 rpm: (left), drop-size number distributions, Run A6 (Table 7); (right), local dispersed-phase holdup profiles, Run A6 (the overall dispersed-phase holdup is represented as that of stage 0).

results of such extrapolations are given in Table 6, after varying the operating variables only one by one.

It becomes obvious that, while the model and its parameters are satisfactorily robust for varying continuous- and dispersed-phase flowrates, for strong decreases in the agitation intensity, at least the dispersed-phase feed distribution and transport ($k_{1\text{Transport}}$) parameters must be revised, taking into account the previously mentioned observations by Tsouris[25] that a less-intensive agitation yields (for the particular distributor used) an overall decrease in the drop diameters and our own observation that, in such conditions (e.g., 100 rpm), some exceptionally large drops may be found at the dispersed-phase feed section.

Thus, we carried out new optimizations, one for each of the new sets of operating conditions, allowing for variations only in the dispersed-phase feed parameters, with the results presented in Table 7 and, for the dispersed-phase local drop-size distribution and holdup profiles, in Figures 8−11.

The obvious improvement of the fits in the most difficult case of decreasing agitation intensity and the way the parameters did change confirm our previous observations—decreased average drop diameter but significantly increased standard deviation, with the ensuing appearance of large drops—a phenomenology that requires incorporation into the model. The higher $k_{1\text{Transport}}$ value found at low agitation speeds also improves the fit.

By contrast, the variations of the optimum dispersed-phase feed parameters with either of the phase flowrates, as well as the corresponding fit improvements, are not significant, which led us to tentatively conclude that, within the ranges explored and in this particular context, the phase flow rates are really not very significant variables. However, for homogeneity and completeness of treatment, the corresponding, only slightly improved, results are also included here.

Conclusions

A new, powerful, and precise algorithm to simulate the hydrodynamic behavior of an agitated liquid−liquid extraction column (Kühni type) has been developed.

The agreement between the local drop-size distributions and the holdup profile obtained experimentally and the values predicted by the model may be considered good. An exception to this fact was observed in the simulated values obtained for a low intensity of agitation. In these low-agitation experiments, the measurement of the drop-size distributions takes a long time, because the low values for dispersed-phase holdup entail a small

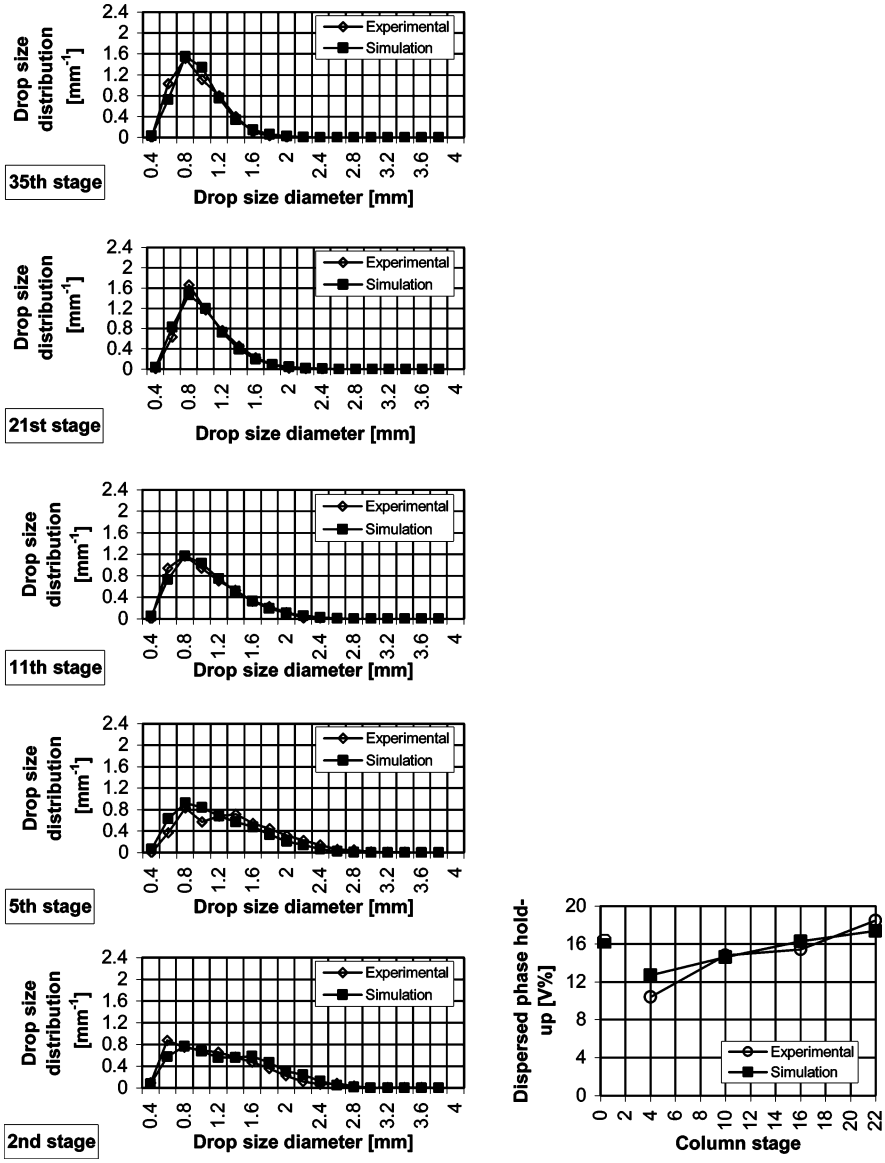

Figure 11. Simulated and experimental values under operating conditions Q_C = 125 L·h^{-1}, Q_D = 176 L·h^{-1}, and 140 rpm: (left), drop-size number distributions, Run A7 (Table 7); (right), local dispersed-phase holdup profiles, Run A7 (the overall dispersed-phase holdup is represented as that of stage 0).

number of drops entering the sampling device per unit time. This is not, however, a typical industrial situation.

Experiments over a broad spectrum of operating conditions have shown that steady-state drop-size distributions result from equilibria between breakage and coalescence processes (in addition to flow processes in continuous operations), so that, despite their computational burden, coalescence (and not just breakage) cannot be neglected when modeling the behavior of agitated liquid−liquid dispersions.

The excellent stability obtained for the values of the interaction and transport model parameters when considering variations of 10% in operating conditions (i.e., continuous- and dispersed-phase flowrates and intensity of agitation) clearly shows that the model is satisfactorily robust.

Acknowledgment

This work was carried out under the gratefully acknowledged financial support of the IPP-Fundo de Apoio à Investigação and the staff of Lehrstuhlfür Fluidverfahrenstechnik, at the University of Munich, Germany.

Nomenclature

$B(\bar{n},t)$ = drop birth term in PBE, appropriate dimensions
C_R = constriction factor, dimensionless
d, d' = drop diameter, m
D = drop death rate
$D(\bar{n},t)$ = drop death term in PBE, appropriate dimensions
D_C = internal column diameter, m
D_R = rotor diameter, m
e = fractional free cross-sectional area (S_e/S), dimensionless
$g(d)$ = drop breakage frequency, s^{-1}
$h(d,d')$= drop collision frequency, s^{-1}
H = compartment height, m
k_{1Break}, k_{2Break} = breakage constants, dimensionless
k_{1Coal} = coalescence constant, m^{-3}
k_{2Coal} = coalescence constant, m^{-2}
$k_{1PowerFact}$ = parameter for the agitation speed-power, dimensionless
$k_{1Transport}$ = parameter for the effective flow area, dimensionless
$k_{2Transport}$ = parameter for the axial dispersion, dimensionless
n = vector of drop properties, appropriate dimensions
N = rotor speed, rev s^{-1}

N_P = power number, dimensionless
P = power input per compartment, W
Q= flowrate, L h^{-1}
Re_R = rotor Reynolds number ($ND_R^2\rho_C/\mu_C$), dimensionless
S = column cross-sectional area, m^2
t = time, s
v_D = radial velocity of the continuous phase, m s^{-1}
V = superficial velocity, m·s^{-1}
$X(\bar{n},t)$ = multivariate drop number density function, appropriate dimensions

Greek Symbols

ϵ = mechanical power dissipation per unit mass, W kg^{-1}
$\lambda(d,d')$ = coalescence efficiency, dimensionless
μ_C = continuous-phase viscosity, Pa s
π = 3.1416
ρ_C = continuous-phase density, kg m^{-3}
ρ_D = dispersed-phase density, kg m^{-3}
$\Delta\rho$ = density difference, kg m^{-3}
σ = interfacial tension, N m^{-1}
ϕ = dispersion phase holdup, dimensionless

Subscripts

C = continuous phase
D = dispersed phase

Literature Cited

(1) Coulaloglou, C. A.; Tavlarides, L. L. Description of Interaction Processes in Agitated Liquid Liquid Dispersions. *Chem. Eng. Sci.* **1977**, *32*, 1289.

(2) Cruz-Pinto, J. J. C. Experimental and Theoretical Modelling Studies of the Hydrodynamic and Mass Transfer Processes in Countercurrent-Flow Liquid−Liquid Extraction Columns. Ph.D. Dissertation, The Victoria University of Manchester, U.K., 1979.

(3) Tsouris, C.; Kirou, V. I.; Tavlarides, L. L. Breakage and Coalescence Models for Drops in Turbulent Dispersions. *AIChE. J.* **1994**, *40*, 395.

(4) Gerstlauer, A.; Mitrovic, A.; Gilles, E. D.; Zamponi, G.; Stichlmair, J. A Detailed Population Model for the Dynamics of Agitated Liquid−Liquid Dispersions. In *Value Adding Through Solvent Extraction*; Shallcross, D. C., Paimin, R., Prvcic, L. M., Eds.; University of Melbourne: Melbourne, Australia, 1996.

(5) Gomes, M. L. A. C. N. Comportamento Hidrodinâmico de Colunas Agitadas de Extracção Líquido-Líquido. Ph.D. Dissertation, Universidade do Minho, Portugal, 1999.

(6) Gomes, L. N.; Guimarães, M. M. L.; Lopes, J. C.; Madureira, C. N.; Stichlmair, J.; Cruz-Pinto, J. J. C. Reproducibility of the Hydrodynamic Performance and Measurements in a Liquid−Liquid Kühni Extraction Column−Relevance to Theoretical Model Evaluation. *Ind. Eng. Chem. Res.* **2004**, *43*, 1061.

(7) Ribeiro, M. M. M.; Guimarães, M. M. L.; Madureira, C. M. N.; Cruz Pinto, J. J. C. Non-Invasive System and Procedures for the Characterization of Liquid−Liquid Dispersions. *Chem. Eng. J.* **2004**, *97*, 173−182.

(8) Ribeiro, L. M.; Regueiras, P. F. R.; Ribeiro, L. M.; Guimarães, M. M. L.; Madureira, C. M. N.; Cruz-Pinto, J. J. C. The Dynamic Behaviour of Liquid−Liquid Agitated Dispersions. I. The Hydrodynamics. *Comput. Chem. Eng.* **1995**, *19* (3), 333.

(9) Ribeiro, L. M.; Regueiras, P. F. R.; Ribeiro, L. M.; Guimarães, M. M. L.; Madureira, C. M. N.; Cruz-Pinto, J. J. C. The Dynamic Behaviour of Liquid−Liquid Agitated Dispersions. II. Coupled Hydrodynamics and Mass Transfer. *Comput. Chem. Eng.* **1997**, *21* (5), 543.

(10) Cruz-Pinto, J. J. C.; Korchinsky, W. J.; Al Husseini, R. Mass Transfer to nonuniform dispersions in countercurrent flow liquid−liquid extraction columns. In *Proceedings of ISEC'83 Conference*; American Institute of Chemical Engineers: Denver, CO, 1983.

(11) Ribeiro, L. M.; Regueiras, P. F. R.; Guimarães, M. M. L.; Cruz-Pinto, J. J. C. Numerical Simulation of Liquid−Liquid Agitated Dispersions on the VAX 6520/VP. *Comput. Syst. Eng.* **1995**, *6*, 465.

(12) Regueiras, P. F. R.; Gomes, M. L.; Ribeiro, L. M.; Guimarães, M. M. L.; Cruz-Pinto, J. J. C. Efficient Computer Simulation of The Dynamics of An Agitated Liquid−Liquid Extraction Column. In *CHEMPOR'98−7th International Chemical Engineering Conference*; Fernando Ramôa Ribeiro, Sebastião S. Alves: Lisboa, Portugal, September 1998; p 765.

(13) JNICT/FCT−Projecto−Jovens Doutorados, Program CD, Faculdade de Engenharia da Universidade do Porto, Portugal, 2000.

(14) Zamponi, G. Das dynamische Verhalten einer gerührten Solvente-extraktionskollonne. Ph.D. Dissertation, Technische Universität München, München, Germany, 1996.

(15) Genenger, B.; Lohrengel, B.; Lorenz, M.; Vogelpohl, A. *Hydromess−Meβsystem zur Bestimmung der Blasen−und Tropfengröβe in Mehrphasenströmungen*; Institut für Thermische Verfahrenstechnik der TU Clausthal: Germany, 1991.

(16) Yi, J.; Tavlarides, L. L. Model for holdup measurements in liquid dispersions using an ultrasonic technique. *Ind. Eng. Chem. Res*. **1990**, *29*, 475.

(17) Godfrey, J. C.; Slater, M. J. *Liquid−Liquid Extraction Equipment*; Godfrey, J. C., Slater, M. J., Eds.; John Wiley & Sons: New York, 1994.

(18) Mišek, T. General Hydrodynamic Design Basis for Columns. In *Liquid−Liquid Extraction Equipment*; Godfrey, J. C., Slater, M. J., Eds.; John Wiley & Sons: New York, 1994.

(19) Goldmann, G. Ermittlung und Interpretation von Kennlinienfelderen einer gerührten Extraktionskolonne. Ph.D. Dissertation, Technische Universität München, München, Germany, 1986.

(20) Tsouris, C. Modelling and control of extraction columns. Ph.D. Dissertation, Syracuse University, Syracuse, NY, 1992.

(21) Kumar, A.; Hartland, S. A Unified Correlation for the Prediction of Dispersed-Phase Hold-Up in Liquid−Liquid Extraction Columns. *Ind. Eng. Chem. Res.* **1995**, *34*, 3925.

(22) Nash, J. C. *Compact Numerical Methods for Computers: Linear Algebra and Function Minimisation*; Adam Hilger: Bristol, U.K., 1979.

(23) Ribeiro, L. M.; Regueiras, P. F. R.; Guimarães, M. M. L.; Cruz-Pinto, J. J. C. Efficient algorithms for the dynamic simulation of agitated liquid−liquid contactors. *Adv. Eng. Software* **2000**, *31*, 985.

(24) Gomes, E. F.; Ribeiro, L. M.; Regueiras, P. F. R.; Cruz-Pinto, J. J. C. A Parallel Algorithm for the Simulation of the Dynamic Behaviour of Liquid−Liquid Agitated Columns. *Proceedings of Vector and parallel processing VECPAR 2000*; LNCS, Springer: New York, 2000.

(25) Guimarães, M. M. L. Processos de interacção e transferência de massa na fase dispersa de Sistemas líquido-líquido. Ph.D. Dissertation, Universidade do Minho, Centro de Química Pura e Aplicada, Braga, Portugal, 1989.

(26) Gomes, M. L. A. C. N.; Guimarães, M. M. L.; Zamponi, G.; Stichlmair, J.; Regueiras, P. F. R.; Cruz-Pinto, J. J. C. The Importance of Drop Coalescence in a Stirred Liquid−Liquid Extraction (Kühni) Column. In *Proceedings of ISEC'99*; Society for Chemical Industry (SCI): Barcelona, 1999.

Received for review December 29, 2005
Revised manuscript received March 11, 2006
Accepted March 29, 2006

IE051453L